

Comprehensive Analysis of Rotor Eccentric Fault in Squirrel Cage Induction Motor – A Review

Shekhawat Narendra M.

Department of Electrical Engineering
Shantilal Shah Engineering College, India

Abstract— Induction motors are the back bone of today's industries. In addition to that squirrel cage induction motors are most used induction motors in today's world. The most common faults occurs in induction motors are mechanical faults in which Eccentric fault represents considerable part. This paper consists of modelling of three phase cage induction motor under the impetration of eccentric fault. A review of Winding Function Approach and Finite Element Method based modelling approach is done to obtain current signature of the motor. The comparison of most common methods is done which used for the modelling of eccentric fault.

Keywords: Induction Motor, Finite Element Method (FEM), Winding Function Approach, Eccentricity

I. INTRODUCTION

Induction motors are rotating electrical machines used in most industrial applications for the conversion of power from electrical to mechanical form. Thus, these are looked upon as the workhorse of Production. The general applications for these motors include pumps, conveyors, machine tools, presses and packaging equipment. Some of these uses are in perilous locations, operating under harsh environments. The significant points of interest in these Motor are that they are very dependable, require low upkeep, and have moderately high productivity. Besides, the wide scope of intensity evaluations, which is from several watts to megawatts, fulfils the generation needs of most mechanical procedures. Now a days the induction motors used in industries operate using inverter drives. In this case, the motor is not directly connected to the power grid but inverter-fed. The inverter provides variable voltage and frequency in order to vary the speed.

However, induction motors are subjected to many types of faults in industrial applications. A motor fault that is not detected at an early stage may become cataclysmic and the induction motor may endure disrupt detriment. Thus, concealed motor faults may grounds motor failure, which in turn may cause production shutdowns. Such Cessation of work are costly, in terms of production time, maintenance cost. Common faults occurring in electrical motor drive systems can be classified as follows:

- Electrical faults: short circuit of stator winding, broken end-ring , broken rotor bar, and inverter faults.
- Mechanical faults: Rotor eccentric fault, shaft alignment problem, faults in bearing, load faults: gearbox fault or general failure in the load parts of the drive, unbalance. The Table 1.1 revealed Percentage incidence of these faults in induction motor. This table shows the assessments were accomplished on 1141 motors by IEEE-IAS [1] and the Electric Powers Research Institute (EPRI) have done assessments on 6312 motors [2]. According to these surveys, most common fault or the

major portion of fault in induction motor was caused by bearing & winding fault.

Faults	Percentages of failures (%)	
	IEEE-IAS	EPRI
Bearing related	44	41
Windings related	26	36
Rotor related	8	9
Others(mainly eccentricity)	22	14

Table 1-1: Percentage failure by component.

Numerous alternatives have been used in industry to inhibit ruthless wound to induction motors. Programmed continuance is implemented to authenticate the straightforwardness of the motor, lubrication inconvenience, bearing state of affairs, stator winding and rotor cage reliability. However, most maintenance is performed with the motor the de-energised, which implies production shutdown. Redundancy is one scheme to put a stop to manufacture shutdowns, but not induction motor collapse. Employing redundancy requires number of pairs of apparatus together with the induction motors, the foremost set operates except there is malfunction where the backup set takes over. This solution is not feasible in many industrial applications due to physical space and high cost limitations.

Air-gap oddity is acknowledged as a state of affairs that take place when there is a no homogeneous void among the rotor and stator in the air-gap. When there is an peculiarity in the air-gap, shifting inductances make happen crooked magnetic flux within the air-gap that generates imperfect harmonics in the line current, which can be acknowledged in the spectrum. There are three varieties of eccentricity faults revealed in Figures:

- 1) Static eccentricity: when stator bore axis and rotor axis are not coincided and but rotor still rotate around its own axis is generally know as static eccentricity as shown in fig.
- 2) Dynamic eccentricity: in this eccentricity both stator and rotor axis are not coincided but the rotation motor is around the stator bore axis
- 3) Mixed eccentricity: When static and dynamic both eccentricity are present simultaneously known as Mixed eccentricity. Here the rotation axis is neither stator nor rotor.

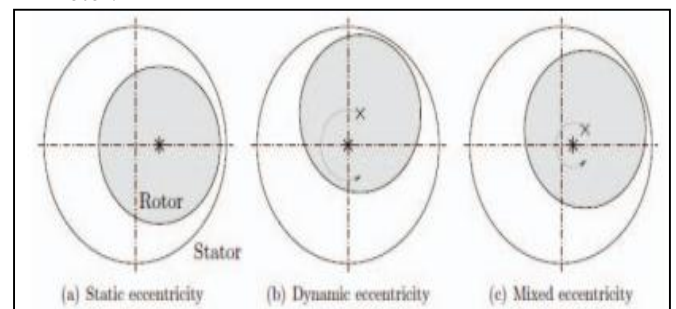


Fig. 1: Types of eccentricity [3]

Circumstance Monitoring and defect recognition improves the consistency and ease of use of the active arrangement. In view of the fact that a range of faults disintegrate moderately, there is a prospective for fault exposure at near the beginning stage. This avoids sudden and total failures which have serious consequences. In the perspective of situation monitoring it is essential to discriminate fault uncovering from fault diagnosis. Fault detection is the decision if the fault is present or not, while fault determination gives more data about the root cause of the failure or localisation of the failure. This data can be utilized to limit vacation and to plan satisfactory upkeep activity. The various diagnosis techniques adopted in industry have been performed mainly through the following strategies [4].

A. *Signal-based fault diagnosis*

- 1) Mechanical vibration analysis.
- 2) Temperature measurement.
- 3) Acoustic noise analysis.
- 4) Electromagnetic field monitoring through inserted coil.
- 5) Instantaneous output power variation analysis.
- 6) Motor current signature analysis (MCSA).

B. *Model-based fault diagnosis.*

- 1) Neural network.
- 2) Fuzzy logic analysis.
- 3) Genetic algorithm.
- 4) Artificial intelligence.
- 5) Finite-element (FE) magnetic circuit equivalents.
- 6) Linear-circuit-theory-based mathematical models.

C. *Fault analysis -based on Machine-theory.*

- 1) Magnetic equivalent circuit (MEC).
- 2) Winding function approach (WFA).
- 3) Modified winding function approach (MWFA).

D. *Fault analysis based on simulations:*

- 1) Finite-element analysis (FEA).
- 2) Time-step coupled finite element state space analysis (TSCFE-SS).

Here in this paper the most two popular methods review is done two find out which one can be most preferable for fault identification. The methods under review are WFA and FEM. The method or approach used for identification of fault is Motor current signature analysis (MCSA).

II. WINDING FUNCTION APPROACH

Electric machine is an electromagnetic device, one of the best way to analyze it is to obtain the electromagnetic field distribution of the machine. This requires solution of Laplace’s or Poisson’s equation, which quit difficult and time consuming even for simple machine construction. Where fault diagnosis requires analysis of harmonics in machine line current, flux, torque, and speed. Analysis of machines with field solvers to identify fault signatures would be tremendously time consuming.

Describing electric machines as group coupled magnetic circuits presents another way of acquire their operating characteristics. The circuit elements are usually

resistances and inductances. Machine inductances are difficult to calculate because it depends on the rotor position. The winding and modified winding function approach (WFA/MWFA) provides the necessary tool to compute these inductances. The approach uses the geometrical data of induction motor and air gap oddity. Winding structure detect the MMF inside machine which is used for the calculation of flux linkage and inductances. Following assumptions are made for analysis of machine:

- 1) Saturation is insignificant.
- 2) Eddy current, friction, and windage losses are small so can be neglected.
- 3) The magnetic material has infinite permeance.
- 4) Slot effects are negligible.

Winding Function approach accounts for all the space harmonics in the machine. The differential equation shown in [5] used for simulation of m phase induction motor with n rotor bar were model is based on coupled circuit model [6] in that paper they have only consider the static eccentricity.

After 1995 the WFA get more attention form researchers different eccentric faults condition were simulated. Dynamic eccentricity is simulated by [7]. And after for the improvement of basic WFA or MWFA some the assumption like that effect of saturation [8-10], skewing[11], slots[12-14] are consider in literature at later point of time. At most the time axial non-uniformity of machine is not considered in modelling and simulation which is often far form the real situation. Only few researcher has consider inclined SE.[15-18] and M.Ojagi has presented a resent paper [19] in which he has consider that modified 2-D winding ruction theory. Presented with simulate axially non-uniform ME and axially uniform ME with experimental inspection.

A. *Multi Coupled Circuit Modeling of Cage Induction Motor*

In this approach all rotor bar are considered as individual loop for the calculation of inductances as shown in fig.

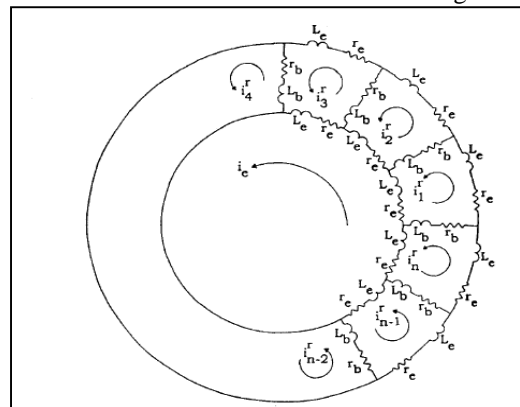


Fig. 2: Equivalent circuit of squirrel cage rotor showing rotor loop currents and circulating end ring current.[6]

Induction motor having a m stator circuit and n rotor bar is under consideration. The cage is seen as n identical equally spaced rotor loop. The equation required for the system modelling are shown bellow :

$$[V_s] = [R_s][I_s] + \frac{d[\psi_s]}{dt} \quad (1)$$

$$[O] = [R_r][I_r] + \frac{d[\psi_r]}{dt} \quad (2)$$

$$[\psi_s] = [L_{ss}][I_s] + [L_{sr}][I_r] \quad (3)$$

$$[\psi_r] = [L_{rs}][I_s] + [L_{rr}][I_r] \quad (4)$$

$$[I_s] = [i_{s1} \ i_{s2} \ \dots \ i_{sm}]^T \quad (5)$$

$$[I_r] = [i_{r1} \ i_{r2} \ \dots \ i_{rm}]^T \quad (6)$$

$$[V_s] = [v_{s1} \ v_{s2} \ \dots \ v_{sm}]^T \quad (7)$$

Where [V] is stator voltage matrix, [I] current matrix, [R] is matrix of resistance and [L] is inductances matrix, [Ψ] is the flux linkage matrix. Subscript s and r represents stator and rotor parameters respectively. The electromagnetic torque and mechanical equation are expressed as following:

$$T_e = \left(\frac{dW_{co}}{d\theta} \right) \Big|_{I_s, I_r = const} \quad (8)$$

$$T_e - T_j = J \frac{d\omega}{dt} \quad (9)$$

$$w = \frac{d\theta}{dt} \quad (10)$$

where T_e is electromagnetic torque of machine, W_{co} is magnetic coenergy, θ is the mechanical angle, T_L is the load torque, J is the inertia of the rotor and ω is the mechanical speed. In a linear magnetic system the coenergy is defined to be

$$W_{co} = 1/2 ([I_s^T][L_{ss}][I_s] + [I_s^T][L_{sr}][I_r] + [I_r^T][L_{rs}][I_s] + [I_r^T][L_{rr}][I_r]) \quad (11)$$

In the case of eccentricity it is easy to show that due to the [L_{rr}] independence of the matrix of space coordinate, the expression for electromagnetic torque is:

$$\tau_e = \frac{1}{2} [I_r^T] \frac{\partial [L_{sr}]}{\partial \theta} [I_s] + \frac{1}{2} [I_s^T] \frac{\partial [L_{rs}]}{\partial \theta} [I_r] + \frac{1}{2} [I_r^T] \frac{\partial [L_{rr}]}{\partial \theta} [I_r] \quad (12)$$

B. Calculation of Inductances and Modelling of eccentricity:

There are three longitudinal axes in induction machines: (1) rotor symmetry axis (A_r), (2) stator symmetry axis (A_s) and (3) rotor rotation axis (A_w). In an ideal case, these three axes coincide and consequently the air gap length is identical and uniform around the stator inner circumference (g_0). Rotation of the rotor does not disturb the uniformity of the air gap as long as slotting is ignored. In practice, these axes may not be coinciding. Wrong rotor positioning or wrong bearing positioning during assembly, bearing wear, misalignment of load and rotor axes, mechanical resonance in critical speed and asymmetry of the mechanical load are some reasons for the eccentricity. Displacement of A_s and A_r disturbs the uniformity of the air gap in the stator inner circumference and an eccentricity fault occurs. The air gap length variation under an eccentricity fault can be described by an air gap function as follows

$$g(\phi, \phi_m, \rho) = g_0 [1 - \cos(\phi - \phi_m)] \quad (13)$$

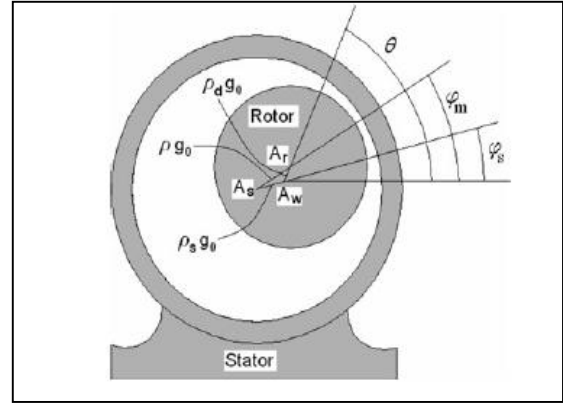


Fig. 3: General eccentricity in a cage induction machine and its parameters [20]

When an eccentricity fault occurs, the position of the A_w axis determines the type of eccentricity. If A_w matches with A_r or A_s , static or dynamic eccentricity occurs, respectively. In a general case, A_w may match neither with A_r nor with A_s . In such a case, mixed eccentricity occurs. In static eccentricity, ρ and Φ_m are constant. In dynamic eccentricity, ρ is constant but Φ_m rotates; its speed is the same as that of the angular velocity of the rotor. In mixed eccentricity, both ρ and Φ_m are rotor position dependent as follows

$$\rho = \sqrt{\rho_s^2 + \rho_d^2 + 2\rho_s\rho_d \cos(\theta - \Phi_s)} \quad (14)$$

$$\phi_m = \phi_s + \tan^{-1} \left(\frac{\rho_s \sin(\theta - \phi_s)}{\rho_s + \rho_d \cos(\theta - \phi_s)} \right) \quad (15)$$

In general maximum limit of ρ is 0 to 1 but due to Unbalanced magnetic pull phenomena it is restricted to 0.75.

Inductances expressed in above equation can be calculated by using winding function theory. The general expression of mutual inductance between two electrical circuit i and j can be expressed as

$$L_{ij}(\theta) = \mu_0 l \int_0^{2\pi} r(\phi, \theta) g_e^{-1}(\phi, \theta) N_i(\phi, \theta) N_j(\phi, \theta) d\phi \quad (17)$$

Where θ is angular position of rotor with respect to some stator reference, Φ is a particular angular position along the stator inner surface, l is the length of the stack, $r(\theta, \Phi)$ is the average radius of air-gap, $g_e^{-1}(\theta, \Phi)$ is termed the inverse gap function and the iron is assumed to be infinitely permeable. The terms $N_i(\theta, \Phi)$ and $N_j(\theta, \Phi)$ are the winding functions of the windings and respectively. Winding function is basically expressed as Fourier series coefficient with turn function and stator slot as shown in below figures.

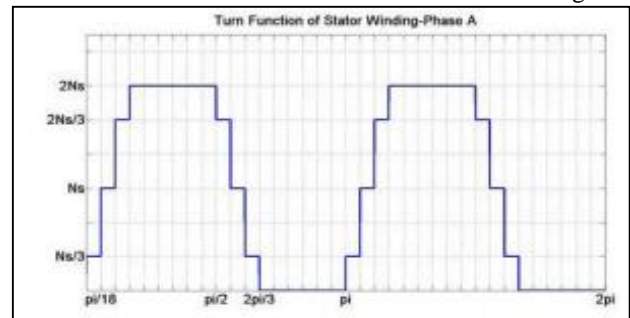


Fig. 4: Turn Function Of stator winding.[21]

III. FINITE ELEMENT METHOD

The basis of any reliable fault diagnosis method of electrical machines is precise performance analysis of them at different conditions. Modelling of faulty machines is the first step of this procedure and has considerable effects on the accuracy of results[22]. The features that are utilized for fault detection are extracted from processing of signals that are simulated at this stage. The modelling approaches that ignore effective characteristics of the machines cannot be used for modelling faulty machines. The two-dimensional (2-D) and three dimensional (3-D) finite element method (FEM) as powerful simulators have been utilized to model faulty machines in different cases. In these methods, spatial distribution of the stator windings, non-uniformity of the air-gap due to stator and rotor slots, non-linearity characteristics of the stator and rotor core materials, skin effects, skewing of the rotor bars, end effects of the stator windings and eddy currents are taken into account[23]. Although all the aforementioned characteristics are taken into account in the 3-D FEM, some of these characteristics, such as skewing of the rotor bars and end effects of the stator windings, are not considered in the 2-D FEM. Moreover, the calculated torque using 2-D FEM is torque per length, which should be multiplied by the motor stack. In these modelling approaches, the field distribution within the machines is determined.

Then, other parameters and variables of the machines such as inductances, currents, the electromotive force (EMF), developed torque, and speed of the machines are calculated. It is noticeable that symmetrical characteristics of the machines may be used to model a quarter or a half of the healthy machines instead of modelling the complete machine. However, this simplification cannot be used in the case of faulty machines.

Based on the supply to the machine, FEMs are classified into current-fed and voltage-fed approaches. In the current-fed approach, an equivalent current density is applied to the coils and then vector potential and flux density are calculated in any area of the machine. It is obvious that this method cannot be employed to compute the stator currents as the most popular signals for processing and feature extraction because on this technique, the stator currents have been supposed to be known values by their equivalent current densities. The time-stepping finite element coupled state space (TSFEM-SS) has been proposed to solve this problem. In this technique, the inductances of the machines are calculated using the current-fed FEM. Then, the resultant inductances are used in the state space equations to determine the other variables and parameters. In most cases, the voltage-fed time-stepping finite element method (TSFEM) has been utilized to calculate machine signals. In this technique, the FE area is coupled to the electrical circuits and mechanical loads. Modelling of faulty induction motors (IMs) using TSFEM has four essential parts. They are geometrical modelling, winding modeling, mechanical coupling, and fault modelling.

A. Geometrical Modeling of Faulty Induction Motors Using Time-Stepping Finite Element Method (TSFEM)

In order to model the geometry of an IM, all parts of the motor, which include the shaft, stator and rotor slots, stator and rotor laminations, are modelled. Then, the physical

characteristics of any part of the motor are applied based on the practical materials used. For instance, in IMs, stator slots are filled by copper, which has evident permeability and conductivity. The rotor slots, which are filled by aluminium with known permeability and conductivity, are short circuited. The B-H curve of the materials used in the stator and rotor cores is taken into account. Figure 3.3 depicts the 2-D stator and rotor laminations of the IM. The 3-D configuration of the same motor has been demonstrated in Figure 3.4.

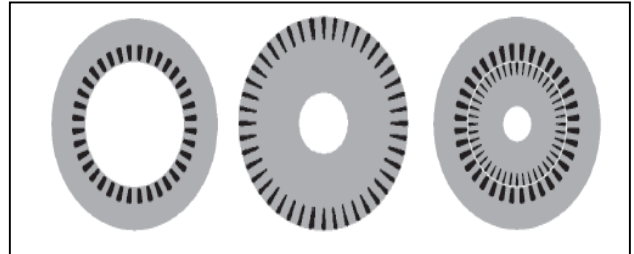


Fig. 5: Cross-section of (left) stator, (middle) rotor, and (right) whole motor.[4]

According to Figure 4 and Figure 5, there are some differences between 2-D and 3-D TSFEMs. It is seen that end effects of the stator windings have been taken into account in 3-D modelling. This characteristic can be modelled in the 2-D FEM using constant inductance in the electrical circuits, which are coupled to the finite element (FE) area.

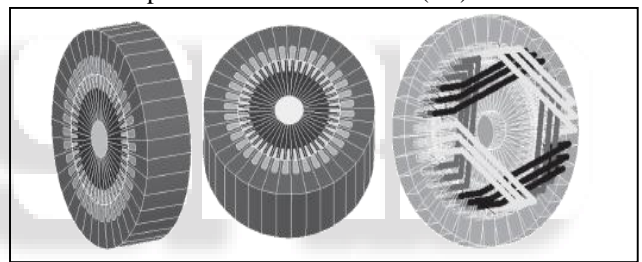


Fig. 6: The 3-D configuration of the motor [4]

B. Coupling of Electrical Circuits and Finite Element Area:

This stage of modelling procedure has considerable impact on the simulation results accuracy. The sinusoidal or non-sinusoidal supply types are determined here. In this stage, the motor is fed by the three-phase sinusoidal supply, unbalanced sinusoidal supply, or inverters. Figure 3.3 illustrates the coupling between electrical circuits and FE area in different supply conditions.

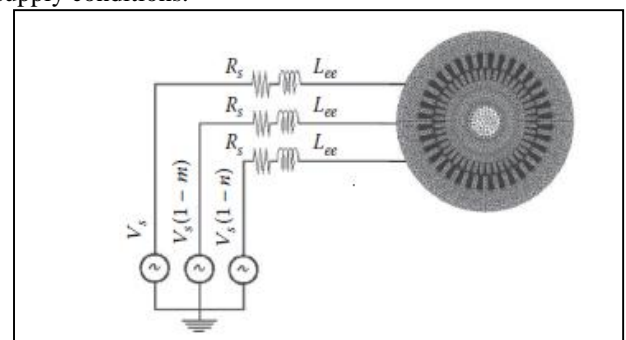


Fig. 7: Coupling electrical circuits to the finite element area.[4]

According to Figure 3.3, the end effects of the stator windings have been modeled using external inductances, which are calculated analytically and added to the electrical

circuits. The transient equations of the external circuit that exhibits the electric supplies and circuit elements are combined to the field equations in FEM. Also, the motion equations due to mechanical coupling are combined to the mentioned previous electromagnetic equations. Solution of these equations yields the magnetic flux density distribution, the stator phase current, the EMF, the developed torque, and speed of the motor. Two-dimensional magnetic field propagation is given as follows:

$$\frac{\partial}{\partial x} \frac{1}{\mu} \left(\frac{\partial A}{\partial x} \right) + \frac{\partial}{\partial y} \frac{1}{\mu} \left(\frac{\partial A}{\partial y} \right) = J_0 + J_e + J_v \quad (3.1)$$

where A is the z-component of the magnetic vector potential, and μ is the magnetic permeability. J_0 is the current density related to the applied voltage, J_e is the current density related to the time variations of the magnetic flux, and J_v is the current density related to the motional voltage. Therefore, Equation (3.1) is rewritten as follows:

$$\frac{\partial}{\partial x} \frac{1}{\mu} \left(\frac{\partial A}{\partial x} \right) + \frac{\partial}{\partial y} \frac{1}{\mu} \left(\frac{\partial A}{\partial y} \right) = -\sigma \frac{V_s}{l} + \sigma \frac{\partial A}{\partial t} + \sigma v \times \nabla \times A \quad (3.2)$$

where σ is the electrical conductivity, l is the motor stack along z-axis, V_s is the applied voltage, and v is the speed of the conductor against magnetic flux density. By applying a reference frame that is assumed fixed in respect to the proposed element, v is equal to zero, and the propagation equation is simplified as follows:

$$\frac{\partial}{\partial x} \frac{1}{\mu} \left(\frac{\partial A}{\partial x} \right) + \frac{\partial}{\partial y} \frac{1}{\mu} \left(\frac{\partial A}{\partial y} \right) = -\sigma \frac{V_s}{l} + \sigma \frac{\partial A}{\partial t} \quad (3.3)$$

The circuit equation of the magnetic coil is given as follows:

$$V_s(t) = R_s i_s(t) + L_{ee} \frac{di_s(t)}{dt} + emf(t) \quad (3.4)$$

where R_s is the stator resistance, i_s is the stator phase current, L_{ee} is the external inductance added to the electrical circuits due to end effects of the stator windings, and emf is the applied voltage to the FE area. By coupling Equation (3.3) and Equation (3.4), the TSFEM is used to obtain the magnetic vector potential, stator currents, and the EMF. The nonlinear equation that can relate the FE equations expressing the electromagnetic fields of the machine with the circuit equations is as follow:

$$[C][A \quad emf \quad i_s]^T + [D] \left[\frac{\partial A}{\partial t} \quad \frac{\partial emf}{\partial t} \quad \frac{\partial i_s}{\partial t} \right]^T = [P] \quad (3.5)$$

where $[C]$ and $[D]$ are the coefficients matrices, $[P]$ is the vector related to the input voltage, and the solution of Equation (3.5) gives $[A]$ and $[i_s]$ as essential signals for analyzing and processing.

C. Modelling of Eccentric Fault

Eccentricity fault is due to bearings fatigue, manufacturing and assembling processes, and other mechanical reasons. In this fault, conformity of the stator axis, rotor axis, and rotor rotating axis are disturbed.

1) Static Eccentricity

In the case of static eccentricity, the rotational axis of the rotor is identical to its symmetrical axis but has been displayed with respect to the stator symmetrical axis. Although the air-

gap distribution around the rotor is not uniform, it is time independent. The static eccentricity degree (δ_{se}) is defined as follows:

$$\delta_{se} = \frac{|O_s O_w|}{g_0} \quad (3.6)$$

where O_s is the stator symmetry center, O_w is the rotor rotation center, and g_0 is the uniform air-gap length. Figure 3.4 illustrates the position of stator and rotor cross-sections in the static eccentricity, where α_s is the initial angle of static eccentricity and vector $O_s O_w$ is the static transfer vector. This vector is fixed for all angular positions of the rotor. The reasons for increasing the eccentricity are bad position of the stator core due to the mounting of the motor. And non-orientation of the stator and rotor centres during the primary maintenance.

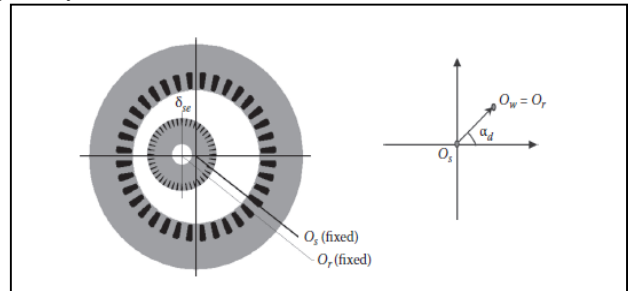


Fig. 8: Geometric configurations of the modeled motor under static eccentricity.[4]

2) Dynamic Eccentricity:

For dynamic eccentricity, the minimum air-gap length depends on the rotor angular position, and it rotates around the rotor. This may be due to misalignment or curvature of the rotor axis. Albeit, the static eccentricity generates asymmetrical magnetic pull, which results in the dynamic eccentricity. In this eccentricity, the symmetry axis of the stator and rotation axis of the rotor is identical, but the rotor symmetry axis has been displaced. In such a case, the air gap around the rotor is non-uniform and time varying. The dynamic eccentricity degree (δ_{de}) is defined as follows

$$\delta_{de} = \frac{|O_s O_w|}{g_0}$$

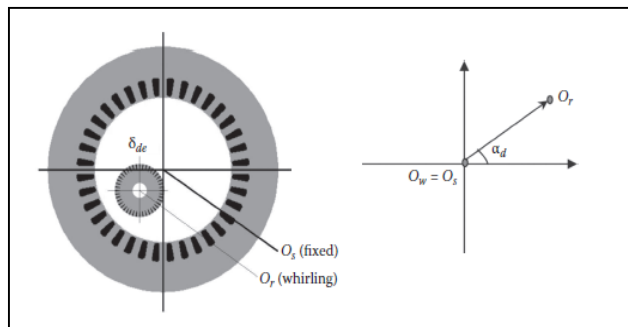


Fig. 9: Geometric configurations of the modeled motor under dynamic eccentricity.[4]

where O_r is the rotor symmetrical axis and vector $O_w O_r$ is the dynamic trans-fer vector. This vector is fixed for all angular positions of the rotor, but its angle varies.

IV. IDENTIFICATION OF ECCENTRIC FAULT BASED ON MCSA

Motor Current Signature Analysis (MCSA) is a condition monitoring technique used to diagnose problems in induction motors, [24-26]. Concept originates from early 1970s and was first proposed for use in nuclear power plants for inaccessible motors and motors placed in hazardous areas, [27]. It is rapidly gaining acceptance in industry today. Tests are performed online without interrupting production with motor running under the load at normal operating conditions, [25,27]. MCSA can be used as predictive maintenance tool for detecting common motor faults at early stage and as such prevent expensive catastrophic failures, production outages and extend motor lifetime. It can be used as a diagnostic tool and powerful addition to vibration and thermal monitoring (verifying a fault with more than one technology), [28-30]. MCSA is method from wider field of Electrical Signature Analysis (ESA), [31], useful for analyzing not only electrical induction motors, but also generators, power transformers as well as other electric equipment. Most popular of these techniques are: Current Signature Analysis (CSA), Voltage Signature Analysis (VSA), Extended Park’s Vector Approach (EPVA) and Instantaneous Power Signature Analysis (IPSA), [32].

Motor Current Signature Analysis is the technique used to analyze and monitor the trend of dynamic energized systems, [28].

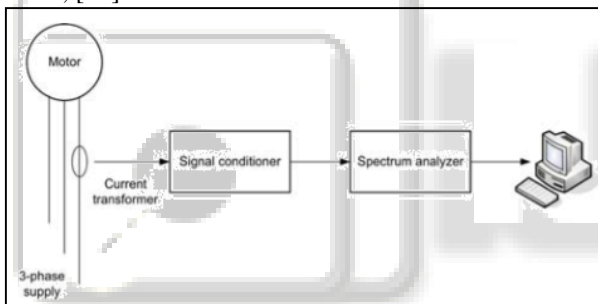


Fig. 10: Stator current monitoring system[24]

MCSA is monitoring stator current or we can say supply current of the motor, [26]. Typical stator current monitoring system is illustrated in Figure 1. Single stator current monitoring system is commonly used (monitoring only one of the three phases of the motor supply current). Current spectrum of a typical induction motor is illustrated in Figure 2. Various electrical and mechanical fault conditions present in the motor further modulate motor current signal and contributes to additional sideband harmonics. Faults in motor components produce corresponding anomalies in magnetic field and change the mutual and self-inductance of motor that appear in motor supply current spectrum as sidebands around line (supply, grid) frequency, [33]. Based on fault signatures motor faults can be identified and its severity accessed. Frequency range of interest in MCSA is typically 0-5 kHz, [28]. This, according to a Nyquist theorem, requires sample rate of at least 10000 samples per second. During the test motor should be run at loading greater than 70%. It should be noted that fault signals detected in motor supply current may also be influenced by operation of neighbouring motors and system’s environmental noise.

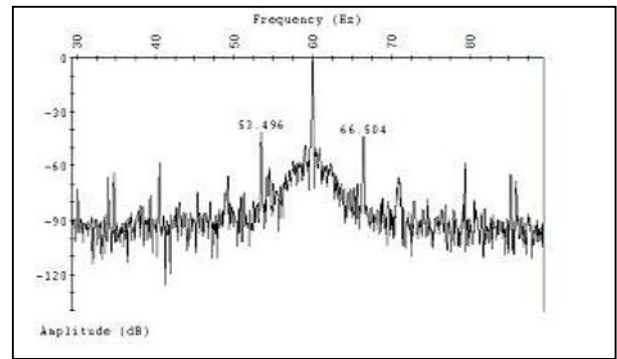


Fig. 11: Current spectrum of induction motor, [34]
Specific Fault Frequency for Eccentricity.

Machine eccentricity is the condition of unequal air gap that exists between the stator and rotor (Heller and Hamata [51], Cameron et al. [52]). When eccentricity becomes large, the resulting unbalanced radial forces (also known as unbalanced magnetic pull or UMP) can cause stator to rotor rub, and this can result in damage of the stator and rotor. There are two types of air-gap eccentricity: the static air-gap eccentricity and the dynamic air gap eccentricity. This misalignment may be because due to several factors such as a bent rotor shaft, bearing wear or misalignment, mechanical resonance at critical speed, etc. Dynamic eccentricity in a new machine is controlled by the total indicated reading (TIR) or “run-out” of the rotor (Barbour and Thomson [53]). An air-gap eccentricity of up to 10% is permissible. However, manufacturers normally keep the total eccentricity level even lower to minimize UMP and to reduce vibration and noise. In reality, both static and dynamic eccentricities tend to co-exist. An inherent level of static eccentricity exists even in newly manufactured machines due to manufacturing and assembly method, as has been reported by Dorrell et al. [38]

The presence of static and dynamic eccentricity can be detected using MCSA [1], [37]. The equation describing the frequency components of interest is

$$f_e = f [(kR \pm n_d) \left(\frac{1-s}{P}\right) \pm v] \quad (16)$$

where $n_d=0$ in case of static eccentricity, and $n_d=1$ in case of dynamic eccentricity (v is known as eccentricity order), f is the fundamental supply frequency, R is the number of rotor slots, s is the slip, P is the number of pole pairs, k is any integer, and v is the order of the stator time harmonics that are present in the power supply driving the motor. In case one of these harmonics is a multiple of three, it may not exist theoretically in the line current of a balanced three-phase machine. However, it has been shown by Nandi et al. [39] and Ferrah et al. [40] that only a particular combination of machine pole pairs and rotor slot number will give rise to significant only static or only dynamic eccentricity-related components. This relationship for a 3-ph integral slot 60 phase belt machine is given by

$$R = 2p[3(m \pm q) \pm r] \pm k \quad (17)$$

Where $m \pm q = 0, 1, 2, 3, \dots$ $r = 0$ or 1 , $k = 1$ or 2 . Simulated results with a four-pole, skewed, 43-rotor slot machine, which conforms to (16) with are given in Fig. 12

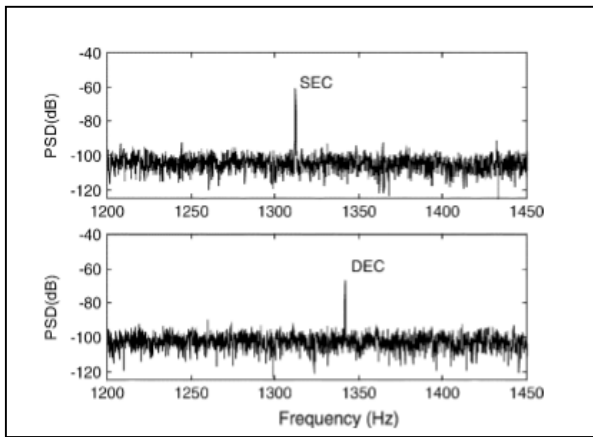


Fig. 12 : Simulated normalized plots of the line current spectra of a 3-ph 3-hp 60-Hz induction motor with 38.46% static (top) and 20% dynamic eccentricity (bottom) with $2p = 4$; $R = 43$. Slip = 0.029 [42]

However, if both static and dynamic eccentricities exist together, low-frequency components near the fundamental [38], [41] given by

$$f_1 = |f \pm kf_r| \quad k=0,1,2... \quad (18)$$

This is shown by Figure 10.

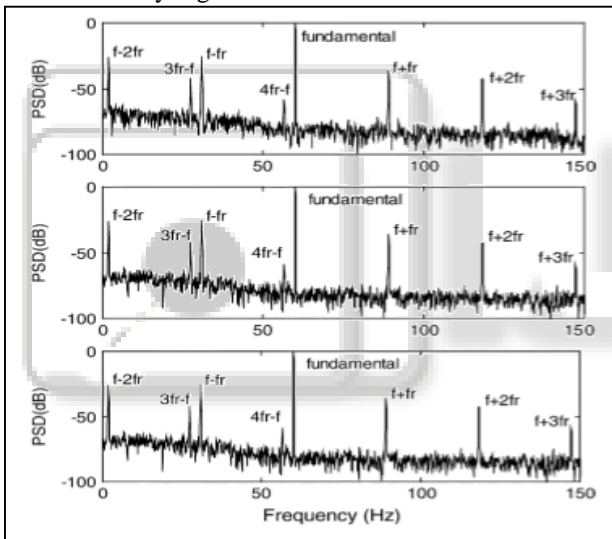


Fig. 13: Simulated, normalized line current spectra of 3-ph 3-hp 60-Hz skewed four-pole induction motors with different rotor slots and identical mixed eccentricity (SE = 38:46%; DE = 20%) machine around fundamental. From top to bottom $R = 44, 43, 42$ slip = 0.029. [42]

V. CONCLUSION

This Paper presents a Modelling of Squirrel cage induction motor under eccentric fault using finite element method and Winding function approach. The fault detection is an important part for condition monitoring of any machinery. Where the eccentric faults are insipient faults which are difficult to detect so for that purpose FEM tool can be used to model the fault. For the detection of this fault a review on Motor current signature analysis is done. In which the current spectrums of stator current is analyzed for the particular fault frequency component. The magnitude of this faulty frequency is observed from which fault is detected successfully. Compression of FEM directly with MWFA

.The results are observed from several paper and found to be very close even though MWFA based model does not include saturation and slotting effects. Also MWFA is found to be less computationally intensive as compared to the FE model. Considering the computational time MWFA based model is definitely more preferable only for the fault identification purpose for actual physical design and analysis FEM is used by professionals.

REFERENCES

- [1] Donnell, P. O., Heising, C., Singh, C. & Wells, S. J. Report of Large Motor Reliability Survey of Industrial and Commercial Installations: Part 3. IEEE Trans. Ind. Appl. IA-23, 153–158 (1987).
- [2] Albrecht, P. F., Apparius, J. C., McCoy, R. M., Owen, E. L. & Sharma, D. K. Assessment of the reliability of motors in utility applications — updated. IEEE Trans. Energy Convers. EC-1, 39–46 (1986).
- [3] Hamid A. Toliyat, Subhasis Nandi, S. C. & Meshgin-kelk, H. Electric Machines Modeling, Condition Monitoring, and Fault Diagnosis. CRC Press (2017). doi:10.1088/1751-8113/44/8/085201
- [4] Luo, X., Lipo, T. A., Liao, Y., Toliyat, H. A. & El-Antably, A. Multiple Coupled Circuit Modeling of Induction Machines. IEEE Trans. Ind. Appl. 31, 311–317 (1995).
- [5] Joksimović, G. M., Durović, M. D., Penman, J. & Arthur, N. Dynamic simulation of dynamic eccentricity in induction machines - winding function approach. IEEE Trans. Energy Convers. 15, 143–148 (2000).
- [6] Toliyat, H. A., Arefeen, M. S., Parlos, A. G. & Member, S. mic Simulation of icity in Induction Machines. Engineer 32, 910–918 (1996).
- [7] Faiz, J. & Tabatabaei, I. Extension of winding function theory for nonuniform air gap in electric machinery. IEEE Trans. Magn. 38, 3654–3657 (2002).
- [8] A. Ghoggal, A. Aboubou, S. E. Zouzou, M. Sahraoui, and H. Razik, “Considerations about the modeling and simulation of air-gap eccentricity in induction motors,” in Proc. IECON 2006, pp. 4987–4992, Nov. 2006.
- [9] K. Ahmadian, and A. Jalilian, “A new method in modeling of rotor bar skew effect in induction motor based on 2D-modified winding function method,” in Proc. IPEC 2007, pp. 630–635, Dec 2007.
- [10] S. Nandi, “Modeling of induction machines including stator and rotor slot effects,” IEEE Trans. Ind. Appl., vol. 40, no. 4, pp. 1058–1065, Jul./Aug. 2004.
- [11] G. Joksimovic, J. Riger, T. Wolbank, N. Peric, M. Vasak, G. Stojvic, and V. Lesic, “Dynamic induction machine model accounting for stator and rotor slotting,” in Proc. ICEM 2012, pp. 207–212, Sept. 2012.
- [12] M. Ojaghi, and S. Nasiri, “Modeling eccentric squirrel-cage induction motors with slotting effect and saturable teeth reluctances,” IEEE Trans. Energy Conversion, vol. 29, no. 3, pp. 619–627, Sept. 2014.
- [13] S. Nandi, “A detailed model of induction machines with saturation extendable for fault analysis,” IEEE Trans. Ind. Appl., vol. 40, no. 5, pp. 1302–1309, Sep./Oct. 2004.
- [14] M. Ojaghi, and J. Faiz, “Extension to multiple coupled circuit modeling of induction machines to include

- variable degrees of saturation effects,” IEEE Trans. Magnetics., vol. 44, no. 11, pp. 4053–4056, Nov. 2008.
- [15] J. Faiz, and M. Ojaghi, “Stator inductance fluctuation of induction motor as an eccentricity fault index,” IEEE Trans. Magnetics., vol. 47, no. 6, pp. 1775–1785, Jun. 2011.
- [16] A. Ghoggal, S. E. Zouzou, M. Sahraoui, H. Derghal, and A. HadriHamida, “A winding function-based model of air-gap eccentricity in saturated induction motors,” in Proc. ICEM 2012, pp. 2739–2745, Sept. 2012.
- [17] A. Ghoggal, S. E. Zouzou, H. Razik, M. Sahraoui and A. Khezzar, “An improved model of induction motors for diagnosis purposes – slot skewing effect and air-gap eccentricity faults,” Energy Conversion and Management, vol. 50, no. 5, pp. 1336-1347, May 2009.
- [18] BL R. Samaga, K. P. Vittal, “Inclined mixed air gap eccentricity detection method for an induction motor,” in Proc. ICAECT 2014, pp. 37-41, Jan. 2014.
- [19] M. Ojaghi and M. Mohammadi, “Modeling eccentricity faults with axial asymmetry in three-phase induction motors,” in Proc. IECON 2016, pp. 1524-1529, Oct. 2016
- [20] T. Ilamparithi, and S. Nandi, “Comparison of modified winding function approach and finite element method results for eccentric salient pole synchronous motor,” in Proc. PEDES 2012, pp. 1–6, Dec. 2012.
- [21] Faiz, J., Ebrahimi, B. M. & Sharifian, M. B. B. Finite element transient analysis of an on-load three-phase squirrel-cage induction motor with static eccentricity. *Electromagnetics* 27, 207–227 (2007).
- [22] Faiz, J., Ebrahimi, B. M., Akin, B. & Toliyat, H. A. Motors Using Finite Element Method. *IEEE Trans. Magn.* 45, 1764–1767 (2009).
- [23] W. T. Thomson and R. J. Gilmore: Motor Current Signature Analysis to Detect Faults in Induction Motor Drives Fundamentals, Data Interpretation, and Industrial Case Histories, Proceeding of the Thirty-Second Turbo machinery Symposium, Houston, Texas, Sept. 2003.
- [24] W. T. Thomson, On-Line Motor Current Signature Analysis Prevents Premature Failure of large Induction Motor Drives, *IME - Maintenance & Asset Management*, Vol. 24, No. 3, May/June 2009, pp. 30-35
- [25] M. El H. Benbouzid, A Review of Induction Motors Signature Analysis as a Medium for Faults Detection, *IEEE Transactions on Industrial Electronics*, Vol. 47, No. 5, Oct. 2000
- [26] A. Korde: On-Line Condition Monitoring of Motors Using Electrical Signature Analysis, Recent Advances in Condition Based Plant Maintenance, 17-18 May 2002, Mumbai.
- [27] H. W. Penrose, The Multi Technology Approach to Motor Diagnostics, 2004, ALLTEST Pro
- [28] D. Miljković, Review Of Machine Condition Monitoring Based On Vibration Data, Proceedings MIPRO 2008 - Vol. III, CTS & CIS, Opatija, Croatia, 2008
- [29] D. V. Ferree and N. Burstein, Electrical Signature Analysis, UltraCheck Diagnostics Grou
- [30] Gheitasi, Motors Fault Recognition Using Distributed Current Signature Analysis, PhD Thesis, Auckland University of Technology, School of Engineering, 2013
- [31] E. L. Bonaldi, L. E. de Lacerda de Oliveira, J. G. B. da Silva, G. Lambert-Torres and L. E. Borges da Silva, Predictive Maintenance by Electrical Signature Analysis to Induction Motors, *Induction Motors – Modeling and Control*, Chapter 20
- [32] Kar and A. R. Mohanty, Monitoring gear vibrations through motor current signature analysis and wavelet transform, *Mechanical Systems and Signal Processing*, Vol. 20, Issue 1, January 2006, pp. 158–187
- [33] A Singhal and M A. Khandekar: Bearing Fault Detection in Induction Motor Using Motor Current Signature Analysis, *International Journal of Advanced Research in Electrical, Electronics and Instrumentation Engineering* Vol. 2, Issue 7, July 2013, pp. 3258-3264
- [34] B. Heller and V. Hamata, *Harmonic Field Effects in Induction Machine*. New York: Elsevier, 1977.
- [35] J. R. Cameron, W. T. Thomson, and A. B. Dow, “Vibration and current monitoring for detecting airgap eccentricity in large induction motors,” *Proc. Inst. Elect. Eng. B*, vol. 133, no. 3, pp. 155–163, May 1986.
- [36] A. Barbour and W. T. Thomson, “Finite element study of rotor slot designs with respect to current monitoring for detecting static air gap eccentricity in squirrel-cage induction motor,” in Proc. IEEE Industry Applications Soc. Annual Meeting Conf., New Orleans, LA, Oct. 5–8, 1997, pp. 112–119.
- [37] D. G. Dorrell, W. T. Thomson, and S. Roach, “Analysis of airgap flux, current, vibration signals as a function of the combination of static and dynamic airgap eccentricity in 3-phase induction motors,” *IEEE Trans. Ind. Appl.*, vol. 33, no. 1, pp. 24–34, Jan./Feb. 1997.
- [38] S. Nandi, S. Ahmed, and H. A. Toliyat, “Detection of rotor slot and other eccentricity related harmonics in a three phase induction motor with different rotor cages,” *IEEE Trans. Energy Convers.*, vol. 16, no. 3, pp. 253–260, Sep. 2001
- [39] A. Ferrah, P. J. Hogben-Liang, K. J. Bradley, G. M. Asher, and M. S. Woolfson, “The effect of rotor design of sensor less speed estimation using rotor slot harmonics identified by adaptive digital filtering using the maximum likelihood approach,” in Proc. IEEE Industry Applications Soc. Annu. Meeting Conf., New Orleans, LA, Oct. 5–8, 1997, pp. 128–135.
- [40] S. Nandi, R. M. Bharadwaj, and H. A. Toliyat, “Performance analysis of a three phase induction motor under incipient mixed eccentricity condition,” *IEEE Trans. Energy Convers.*, vol. 17, no. 3, pp. 392–399, Sep. 2002
- [41] Nandi, S. & Toliyat, H. A. Condition monitoring and fault diagnosis of electrical machines-a review. 20, 197–204 (2003).